SPACE VECTOR-BASED ANALYTICAL ANALYSIS OF THE INPUT CURRENT DISTORTION OF A THREE-PHASE DISCONTINUOUS-MODE BOOST RECTIFIER SYSTEM

JOHANN W. KOLAR, HANS ERTL, FRANZ C. ZACH
Technical University Vienna, Power Electronics Section, Gusshausstrasse 27,
A-1040 Vienna, AUSTRIA

Phone: (int)43 222 58801-3886 Fax: (int)43 222 5052666

Abstract

In this paper the low frequency harmonic distortion of the mains current of a three-phase single-switch discontinuous-mode boost-rectifier is calculated. The system analysis is based on application of space vector calculus and on substitution of discontinuous time shapes within a pulse period by quasi-continuous time shapes. The quasi-continuous time shapes are defined by averaging over the pulse period. The dependency of the shape of the input currents on the voltage transformation ratio is given for various control methods in analytical form. The results of the theoretical analysis are veryfied by digital simulation and by measurements on a laboratory model. A good consistency of the results has been found.

1 Introduction

Today in most cases uncontrolled three-phase bridge circuits are used for coupling of converter systems with voltage DC link to the three-phase mains. Such converters of usually low and medium power are used widely in the industrial automation and process technology.

Regarding the mains behavior this concept is characterized by the presence of high low-frequency mains current harmonics especially for direct mains connection (without smoothing inductances on AC or DC side) or discontinuous conduction of the diode bridge, respectively. Besides higher transmission losses these currents result in a distortion of the mains voltage due to the inner impedance of the supplying mains. This voltage distortion at the point of common coupling may cause an influence or malfunction of other systems. A further basic disadvantage of uncontrolled rectification is that the output voltage is in direct dependency on the voltage of the supplying mains. The mains voltage tolerance band therefore has to be considered for the dimensioning of the load side converter by increasing the VA-rating. Furthermore, a system operation for very much different nominal mains voltages is only possible by using a matching transformer which results in increased system weight and size.

In [1] a three-phase pulse rectifier system (a three-phase discontinuous-mode boost rectifier, cf. **Fig.1**) is introduced which shows a remarkably simple structure of the power and control circuits. As compared to uncontrolled rectification with line commutation, this system also has the advantage of controllable output voltage besides low distortion of the input current. Furthermore, it results in an approximately resistive mains load behavior. The system analysis given in [1] using a single-phase equivalent circuit is limited to high values of the output voltage (related to the mains voltage). This means that the converter operation is not treated by this method in the case of the especially interesting region of an output voltage $U_O = 620\text{V} \ldots 820\text{V}$. This output voltage is a possible DC link voltage level, e.g., for PWM inverter systems for operation from the European low-voltage mains with 380V_{rms} line-to-line voltage.

The analysis of the low-frequency mains current harmonics for the circuit given in [1] are the topic of this paper. The calculation of the power factor is omitted due to the relative low significance regarding the influence on the mains. The importance especially of the low-frequency current harmonics for the judgement of the influence on the mains is due to the high low-frequency harmonic content of the public mains whose limitation based on recommendations (IEEE 519) and regulations (IEC 555-2) is strived for.

The analysis of the system behavior is performed based on the space vector calculus which allows a direct and clear mathematical description of three-phase systems. This avoids the use of a single-phase equivalent circuit as used in [1] which shows only a limited validity. The mains currents remaining after filtering out the high-frequency harmonics of the discontinuous input currents of the rectifier are calculated in analytically closed form. There, a local averaging is used which is related to one pulse period. For pulse frequencies being sufficiently higher than the mains frequency, this approximation shows high accuracy. The time shape and the low-order mains current harmonics are shown graphically for different control methods in dependency on the converter voltage transfer ratio. Finally, the results of the theoretical analysis are verified by digital simulation and by measurements on a laboratory model. A good consistency of the results is obtained.

2 Principle of Operation

As already mentioned, the system of Fig.1 shows the structure of a three-phase single-switch discontinuous-mode boost converter. It can be regarded as being built up based on a three-phase extension of a boost converter [2] as applied for power factor correction of single-phase unidirectional AC-DC power conversion. For low dynamics and constant pulse frequency f_P the control of the converter is performed with an on-time $t_{\mu,1}$ of the power transistor T being approximately constant over the fundamental period. A synchronisation of f_P and mains frequency f_N is not necessary for $f_P \gg f_N$. The output voltage has a lower limit according to the boost converter structure as given by the amplitude of the mains line-to-line voltage $\sqrt{3}\hat{U}_N$.

For illustrating the principle of operation in **Fig.2**, the conduction states of the converter are shown within a pulse period $t_\mu \in [0, T_P]$. Regarding the values of the mains phase voltages we assume $u_{N,R} > 0$, $u_{N,T} \leq u_{N,S} \leq 0$ as being valid for an interval $\pi/6$ of the fundamental period. The mains phase voltages $u_{N,(RST)}$ are considered approximately constant within a pulse period. Due to the low-pass characteristic of the mains filter L_N, C_N, the mains voltage can be thought to be present directly on the filter output. Before transistor T is turned on we have $i_{U,R} = i_{U,S} = i_{U,T} = 0$ according to the discontinuous conduction mode. The DC output voltage u_O is assumed to be sufficiently higher than the peak value of the line-to-line mains voltage.

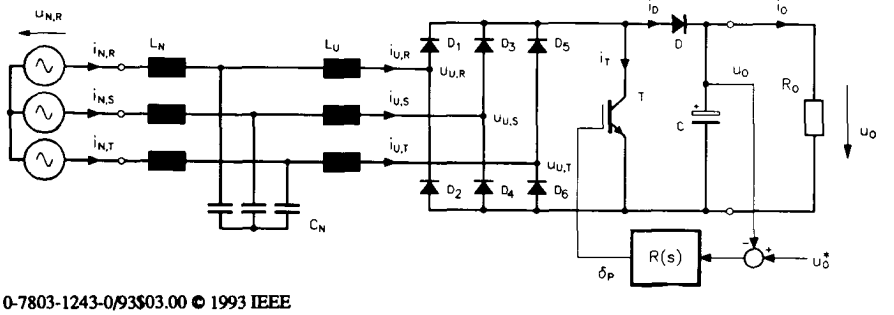

Fig.1: Structure of the power circuit of a three-phase discontinuous-mode boost rectifier. Filtering of the high-frequency spectral components of the discontinuous input currents $i_{U,(RST)}$ of the three-phase diode bridge by mains filter L_N, C_N. The supplying mains is replaced by a star-connection of ideal voltage sources $u_{N,(RST)}$. The relative on-time δ_T of the power transistor T shall be given by a controller $R(s)$ in dependency on the output voltage control error.

0-7803-1243-0/93$03.00 © 1993 IEEE

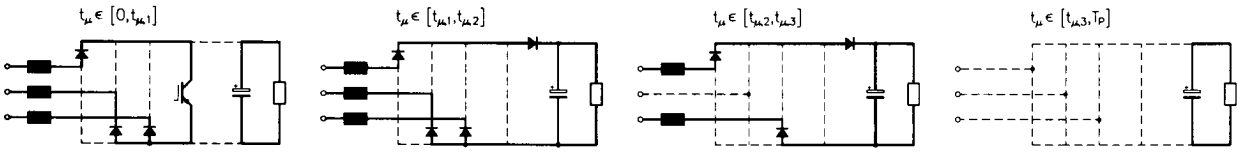

Fig.2: Sequence of the conduction states of a three-phase single-switch discontinuous-mode boost rectifier within a pulse period $t_\mu \in [0, T_P]$ for $u_{N,R} > 0$, $u_{N,T} \leq u_{N,S} \leq 0$. t_μ denotes a local time running within the pulse period. The position of the considered pulse interval within the fundamental period is determined by the global time t or by the phase angle $\varphi_N = \omega_N t$ (ω_N = angular speed of the mains), respectively.

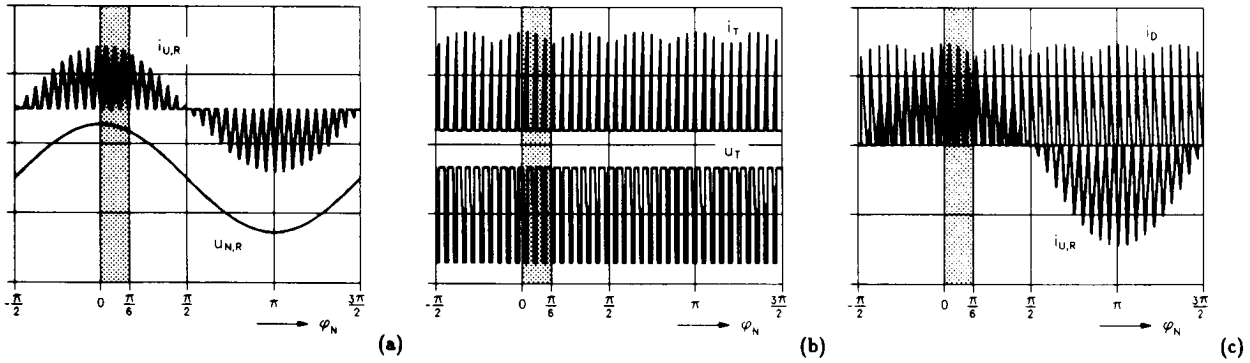

Fig.3: Digital simulation of a three-phase discontinuous-mode boost rectifier without mains filter L_N, C_N, operated with constant switching frequency f_P. Turn-on interval $T_\mu \in [0, t_{\mu,1}]$ constant over the fundamental period; representation for one fundamental period $\varphi_N \in [-\frac{\pi}{2}, \frac{3\pi}{2}]$; dotted area: angle interval $\varphi_N \in [0, \frac{\pi}{6}]$ considered for the analysis of the system behavior; (a): input phase current $i_{U,R}$ (40A/div) and related mains voltage $u_{N,R}$ (400V/div); (b): current i_T through transistor T (25A/div) and voltage u_T across T (600V/div); (c): current i_D through output diode D and current $i_{U,R}$ (both 25A/div); parameters: $U_{N,rms} = 220$V, $U_O = 820$V, $f_N = 50$Hz, $f_P = 1/T_P = 1.95$kHz, $L_U = 1.5$mH, $P_O = 7.5$kW.

Therefore, we have the output diode D and the diodes $D_1 \ldots D_6$ of the three-phase bridge rectifier in blocking state.

T shall be turned on at $t_\mu = 0$. The rate of rise of the phase currents due to the short circuit of the diode bridge on the DC side is defined by the driving mains phase voltages and by the inductances L_U. The turn-off of T in $t_{\mu,1}$ (as given by the control circuit) is followed by demagnetisation of the inductances L_U via diode D into the capacitor C buffering the output voltage. There, only within the first demagnetisation interval $t_\mu \in [t_{\mu,1}, t_{\mu,2}]$ all phases conduct current. In $t_{\mu,2}$ that phase current which shows the smallest absolute value at $t_{\mu,1}$ becomes 0 (in our case, $i_{U,S}$). The following second demagnetisation interval (demagnetisation of the remaining phases R and T which conduct equal currents with opposite signs) is finished at $t_{\mu,3}$. There, one has to guarantee $t_{\mu,3} \leq T_P$ for discontinuous mode by appropriate dimensioning of L_U. Therefore, the system can be analysed only by a rough approximation using a single-phase equivalent circuit because this basically does not include the second demagnetisation interval.

Figure 3 shows the shape of input current $i_{U,R}$ and mains phase voltage $u_{N,R}$ of a three-phase boost-rectifier gained by digital simulation. For demonstration purposes the system is pulsed with low switching frequency. The discontinuous input phase currents $i_{U,(RST)}$ follow envelopes which are proportional to the respective phase voltages $u_{N,(RST)}$. By filtering out the spectral components having switching frequency by a mains filter L_N, C_N connected in series (cf. Fig.1) we therefore obtain an approximately ohmic mains loading (referred to the fundamentals of the mains currents $i_{N,(RST)}$). One has to point out that due to the on-time of T being constant over the fundamental period the current guidance results directly from the mains voltage and not from a sinusoidal variation of the duty cycle of T.

Prior to the calculation of the low-frequency harmonics of the mains currents (cf. section5) remaining after filtering we want to compile the assumptions made there, the definitions and the basics of the calculation method in the following.

3 Analysis Method

3.1 Assumptions

The analysis of the power electronic system is based on the following simplifying assumptions:

- purely sinusoidal, symmetric mains voltage system $u_{N,(RST)}$
- the ripple of the voltages across the filtering capacitors C_N is negligible ($< 10\%$)
- the amplitudes of the fundamental voltage drops across the filtering inductances L_N are negligible as compared to the amplitude of the mains phase voltages $\hat{U}_N$; the voltages across C_N therefore are assumed to be impressed and equal to the mains phase voltages $u_{N,(RST)}$
- constant output voltage u_O (ripple $< 5\%$)
- constant output current I_O
- $f_P > 200 f_N$ or $T_P \ll T_N$, respectively (mains voltages approximately constant within a pulse period)
- ideal system components, especially neglection of losses, switching times etc.

It is of special importance to assume a sufficiently high switching frequency of the converter ($f_P \gg f_N$). As described in the following, this assumption allows a direct analytical calculation of the shape of the filtered converter input current.

According to the phase-symmetric structure of the power electronic system and to the assumed symmetry of the mains voltage we can limit the description of the system behavior as given in section 4 to the interval $\varphi_N \in [0, \frac{\pi}{6}]$ (cf. Fig.3). By simple symmetry considerations this interval can be extended to the entire fundamental period (cf. section 3.2, Eq.(2)).

3.2 Quasi-Continuous Approximation

For a practical realisation of the system one should strive for $f_P > 20$kHz, i.e., above the audible spectrum. A further increase of f_P results in a reduced filtering effort. This seems to be realisable also for higher output power P_O because the discontinuous mode avoids a stress of T due to the reverse recovery current of D.

Based on the the assumption of a high f_P a quasi-continuous analytical approximation

$$i_{N,(RST)}(\varphi_N) = i_{U,(RST),avg} = \frac{1}{T_P} \int_0^{T_P} i_{U,(RST)}(t_\mu)\, dt_\mu \qquad (1)$$

of the mains currents can be calculated [3], [4], [5]. This is achieved by using an averaging of the discontinuous currents $i_{U,(RST)}$. The averaging

suppresses local variations with switching frequency. There, t_μ denotes a local time running within the pulse period, φ_N gives the position of the pulse interval within the fundamental period.

Due to the assumed symmetry of the mains voltage system the shape of, e.g., $i_{N,R}$ within $\varphi_N \in [\frac{\pi}{6}, \frac{\pi}{2}]$ can be given directly by

$$i_{N,R} = \begin{cases} -i_{U,T,avg}(\frac{\pi}{3} - \varphi_N) & \varphi_N \in [\frac{\pi}{6}, \frac{\pi}{3}] \\ -i_{U,S,avg}(\varphi_N - \frac{\pi}{3}) & \varphi_N \in [\frac{\pi}{3}, \frac{\pi}{2}] \end{cases} \quad (2)$$

via an appropriate shift of the shapes of the phase currents $i_{N,S}$ and $i_{N,T}$ which have been calculated for the analysed interval $\varphi_N \in [0, \frac{\pi}{6}]$.

As a check by digital simulation (cf. section 6) shows, for $f_P \geq 500 f_N$ the deviation remains below 1% as compared to the exact values of the low-frequency harmonics of $i_{N,(RST)}$.

Besides the shape of the mains current, also the mean value of the output diode current which defines the output power of the system according to

$$P_O = U_O \, I_{D,avg} \quad (3)$$

can be given in analytically closed form

$$I_{D,avg} = \frac{6}{\pi} \int_0^{\frac{\pi}{6}} i_{D,avg}(\varphi_N) \, d\varphi_N \quad (4)$$

(also shown in section 5). Analogous to Eq.(1) we have for the local mean value of the diode current for the considered angle interval $\varphi_N \in [0, \frac{\pi}{6}]$ (cf. Fig.5):

$$i_{D,avg} = \frac{1}{T_P} \int_{t_{\mu,1}}^{T_P} i_R(t_\mu) \, dt_\mu \, . \quad (5)$$

3.3 Space Vectors

The space vector calculus [6] is used for special clearness and due to a simpler calculation (compared to the methods using phase quantities).

For the definition of the complex phasor associated with a triple of phase quantities we have (for the example of the converter input currents):

$$\underline{i}_U = (i_{U,\alpha} + j \, i_{U,\beta}) = \frac{2}{3} (i_{U,R} + \underline{a} i_{U,S} + \underline{a}^2 i_{U,T}) \qquad \underline{a} = (-\frac{1}{2} + j\frac{\sqrt{3}}{2}) . \quad (6)$$

Remark: Space vectors are used for the description of space distribution of electrical and magnetic quantities in the area of three-phase AC machines. Here, however, formally equal defined complex phasors describe the *time-behavior* of the phase quantities. One should call the complex quantity defined by Eq.(6) therefore correctly a *three-phase phasor* of the instantaneous values of the input currents $i_{U,(RST)}$ of the diode bridge. Because the literature of power electronics does not make a difference between these two aspects, we also will use the term "space vector" in the following.

For the back-transformation of the space vector components $i_{U,\alpha}$ and $i_{U,\beta}$ into phase quantities there follows:

$$i_{U,R} = i_{U,\alpha} \qquad i_{U,S} = -\frac{1}{2} i_{U,\alpha} + \frac{\sqrt{3}}{2} i_{U,\beta} \qquad i_{U,T} = -\frac{1}{2} i_{U,\alpha} - \frac{\sqrt{3}}{2} i_{U,\beta} \quad (7)$$

3.4 Normalization

For a wide applicability and a simple transfer of the relationships derived here, we want to agree on the following normalizations:

$$t_{\mu,i,r} = \frac{1}{T_P} t_{\mu,i} \qquad u_{i,r} = \frac{1}{U_O} u_i \qquad i_{i,r} = \frac{1}{I_n} i_i \qquad p_{i,r} = \frac{1}{P_n} p_i \quad (8)$$

Into the basis quantities

$$I_n = \frac{2}{3} U_O \frac{T_P}{L_U} \qquad P_n = \frac{2}{3} U_O^2 \frac{T_P}{L_U} \quad (9)$$

we include the parameters which directly influence the system behavior. If one includes the output voltage (being controlled to a fixed value) instead of, e.g., the mains phase voltage amplitude into the normalisation basis of currents and powers one can avoid a change of the basis quantities for changing mains voltage conditions (due to the input voltage tolerance band or different nominal values of $\hat{U}_N$).

With Eqs.(3,8,9) we have for the rated system output power:

$$P_{O,r} \equiv I_{D,avg,r} \quad (10)$$

3.5 Definitions

In the following the definitions of important characteristic system quantities are summarised briefly. For the characterization of the system voltage transfer ratio the ratio of output voltage to the amplitude of the mains line-to-line voltage is used according to

$$M = \frac{U_O}{\sqrt{3}\hat{U}_N} \qquad M \geq 1 \, . \quad (11)$$

For the relative on-time of the transistor T we define:

$$\delta_P = \frac{t_{\mu,1}}{T_P} \, . \quad (12)$$

The mains load (regarding the fundamental) and the input characteristic are described by the equivalent input resistance R_N (equivalent star connection; [7], [8]). Considering the power balance

$$P_O = U_O I_{D,avg} = \frac{3}{2} \hat{U}_N \hat{I}_{N,(1)} = \frac{3}{2} \frac{\hat{U}_N^2}{R_N} \, , \quad (13)$$

the relations given in section 3.4 and Eq.(11) there follows:

$$R_N(M, \delta_P) = \frac{3}{4} \frac{L}{T_P} M^{-2} I_{D,avg,r}^{-1} \, . \quad (14)$$

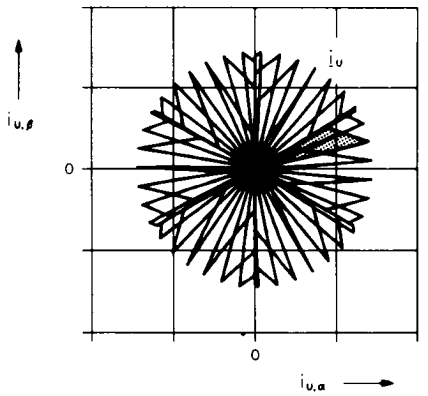

Fig.4: Trajectory of $\underline{i}_U$ related to Fig.3 (25A/div); representation for one fundamental period; within each pulse period a trajectory segment describes an acute-angled triangle (marked by the dotted area).

4 Basic System Equations

According to Eq.(1), the calculation of the local mean values $i_{N,(RST)}$ defining the shape of the mains currents is related to the shape of the discontinuous input currents $i_{U,(RST)}(t_\mu)$ of the bridge rectifier. Its analysis is the topic of this section.

As can be seen from **Fig.4**, the trajectory of $\underline{i}_U$ describes an acute-angled triangle within each pulse period. The mathematical description of these trajectory segments which completely describe the shape of the phase currents within the pulse period according to section 3.1 can be limited to $\varphi_N \in [0, \frac{\pi}{6}]$ (cf. **Fig.5**). The assumed symmetric and purely sinusoidal system of mains voltages

$$u_{N,R} = \hat{U}_N \cos(\varphi_N) \quad u_{N,S} = \hat{U}_N \cos(\varphi_N - \frac{2\pi}{3}) \quad u_{N,S} = \hat{U}_N \cos(\varphi_N + \frac{2\pi}{3}) \quad (15)$$

is described by the mains voltage space vector (rotating with constant angular speed ω_N)

$$\underline{u}_N = \hat{U}_N \, \exp(j\varphi_N) \qquad \varphi_N = \omega_N t \, . \quad (16)$$

$\underline{u}_N$ is approximated by a phasor being fixed within the considered pulse period. Due to the discontinuous operation we have $\underline{i}_U = 0$ before T is turned on in $t_\mu = 0$. The linear rate of rise of the phase currents within $t_\mu \in [0, t_{\mu,1}]$ (cf. Fig.5, right hand side) corresponds to a linear rise of the magnitude of the space vector $\underline{i}_U$ in the direction of $\underline{u}_N$. After turning off T at $t_{\mu,1}$ the voltage space vector defining the current change is given by $\underline{u}_N - \underline{u}_{U,[100]}$ ($\underline{u}_{U,[100]}$: space vector of converter input voltages when diodes D_1, D_4 and D_6 are conducting). When $\underline{i}_U$ reaches the limit $i_{U,S} = 0$ at $t_{\mu,2}$ (i.e., when the phase current showing the smallest absolute value at $t_{\mu,1}$ becomes 0), the second demagnetisation interval begins. From now on the current-driving voltage is given only by the projection of $\underline{u}_N - \underline{u}_{U,[100]}$ onto the axis $i_{U,S} = 0$. The demagnetisation of the inductances L_U is finished at $t_{\mu,3}$. For discontinuous operation one has to guarantee $t_{\mu,3} \leq T_P$ therefore.

Remark: The considerations made show clearly the only limited validity of a system analysis based on a single-phase equivalent circuit. There, a second

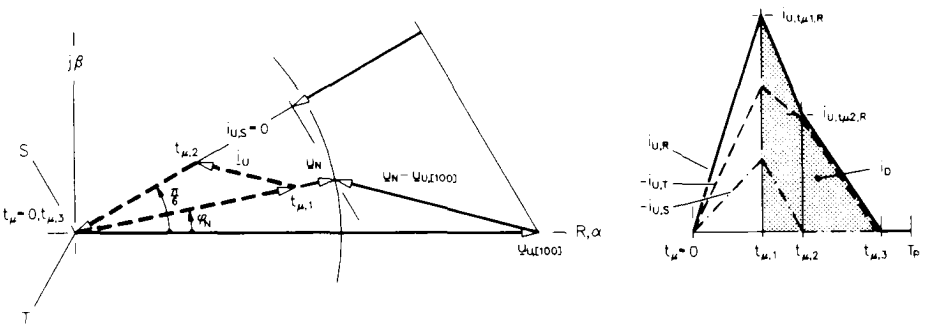

Fig.5: Description of the operating behavior by space vector calculus: trajectory of i_U and related time shape of the converter input currents $i_{U,(RST)}$ and of output diode current i_D (marked by the dotted area) within one pulse period $t_\mu \in [0, T_P]$ for $u_{N,R} > 0$, $u_{N,T} \leq u_{N,S} \leq 0$ (cf. Fig. 2); $\underline{u}_N$: space vector of the mains phase voltages; $\underline{u}_{U,[100]}$: space vector of the input voltages of the three-phase diode bridge when diodes D_1, D_4 and D_6 are conducting (cf. Fig.1); phase $\varphi_N = \omega_N t$ defines the time position of the pulse interval considered within the fundamental period $\varphi_N \in [-\frac{\pi}{2}, \frac{3\pi}{2}]$; parameter: $M = 1.5$.

demagnetisation phase is basically not included. Therefore, especially for small values of M (≤ 2) considerable errors in modelling result.
Considering the differential equation

$$L_U \frac{di_U}{dt_\mu} = \underline{u}_N - \underline{u}_U(i_U, t_\mu) \tag{17}$$

of the AC side system part there follows for the space vector components and time intervals ($\Delta t_{\mu,ji} = t_{\mu,j} - t_{\mu,i}$) defining the trajectory of i_U (consisting of approximately straight line segments):

$$t_\mu = t_{\mu,1}: \quad i_{U,t\mu1,\alpha,\tau} = \frac{\sqrt{3}}{2}\delta_P M^{-1}\cos(\varphi_N)$$
$$i_{U,t\mu1,\beta,\tau} = \frac{\sqrt{3}}{2}\delta_P M^{-1}\sin(\varphi_N) \tag{18}$$

$$t_\mu = t_{\mu,2}: \quad i_{U,t\mu2,\alpha,\tau} = \frac{3}{2}\delta_P M^{-1}\frac{\sin(\varphi_N)}{1+\sqrt{3}M^{-1}\sin(\varphi_N - \frac{\pi}{6})}$$
$$i_{U,t\mu2,\beta,\tau} = \frac{\sqrt{3}}{2}\delta_P M^{-1}\frac{\sin(\varphi_N)}{1+\sqrt{3}M^{-1}\sin(\varphi_N - \frac{\pi}{6})} \tag{19}$$

$$\Delta t_{\mu,21,\tau} = \sqrt{3}\,\delta_P M^{-1}\frac{\sin(\frac{\pi}{6} - \varphi_N)}{1+\sqrt{3}M^{-1}\sin(\varphi_N - \frac{\pi}{6})} \tag{20}$$

$$\Delta t_{\mu,32,\tau} = 2\,\delta_P M^{-1}\frac{\sin(\varphi_N)}{(1+\sqrt{3}M^{-1}\sin(\varphi_N - \frac{\pi}{6}))(1 - M^{-1}\cos(\varphi_N - \frac{\pi}{6}))}$$

The local current flow interval of the three-pase rectifier bridge related to the turn-on time of T results as:

$$\delta^{-1} = \frac{t_{\mu,3}}{t_{\mu,1}} = \frac{1}{1 - M^{-1}\cos(\varphi_N - \frac{\pi}{6})}. \tag{21}$$

Somewhat surprisingly there follows a relationship being valid in an analog manner for DC-DC boost converters. In the case at hand only the (constant) input voltage of the DC-DC converter related to the output voltage has to be replaced by the three-phase rectified mains voltage (for $\varphi_N \in [0, \frac{\pi}{6}]$: $u_{N,RT,\tau} = u_{N,R,\tau} - u_{N,T,\tau} = M^{-1}\cos(\varphi_N - \frac{\pi}{6})$; cf. also [9], Eq.(8)).

5 Mains Current Harmonics

The analyses of the operation of three-phase single-switch discontinuous-mode pulse rectifiers given in the literature are limited to the same control method, i.e., the control with constant turn-on time $t_{\mu,1}$ and constant pulse frequency f_P [1], [8], [9].

The aim of this chapter is to calculate the mains current quality in dependency on M for various control methods. As a basis we have the situation given for constant $t_{\mu,1}$ of T and constant f_P. This control method, to be called **control method I** is given for practical system realization only at the limit of a cut-off frequency of the output voltage control lying substantially below $6f_N$ (or in the case of an open-loop system control).

As a further control method (**control method II**) the operation of the converter is analyzed at the border of the discontinuous mode. Furthermore, again $t_{\mu,1}$ shall be constant over the fundamental period. Turning on of T in this case takes place immediately after the end of the demagnetization interval at $t_{\mu,3}$. Due to the avoidance of a current gap $t_\mu \in [t_{\mu,3}, T_P]$ characterizing the discontinuous operation with constant f_P, maximum utilisation of the power circuit components is achieved. The modulation of the pulse frequency with six times f_N (cf. Fig.7) furthermore leads to a broader distribution of the high-frequency spectral components of $i_{U,(RST)}$. Due to the more even distribution of the same spectral power compared to constant f_P the filtering effort in order to satisfy the regulations for conducted electromagnetic influence (e.g., VDE 0871) is reduced especially for the region **10kHz** $< f <$ **150kHz** [10].

As mentioned, the operation of the system with constant $t_{\mu,1}$ is given only for the case of low dynamics (and if constant load current is assumed). This case is not very important for industrial applications. For high cut-off frequency of the control of u_O (**control method III**) the power oscillations with frequencies with $6i$ ($i = 1, 2, 3, \ldots$) times f_N (which occur on the DC side for constant $t_{\mu,1}$ and constant f_P) are compensated via variation of $t_{\mu,1}$. This results ideally in a constant instantaneous local mean value $p_{O,avg}$ of the output power. If no buffering of load pulses, no buffering during voltage dips and no limitation of mains overvoltages is required, C (which usually would be an electrolytic capacitor) can be realised as a foil-type capacitor. This will have higher current carrying capability, may have much lower C and higher lifetime. This also increases the reliability of the converter [11].

Remark: As shown in [5], Eq.(57), an increase of the output voltage control dynamics in single phase AC-DC converters leads to an increase of the low-frequency spectral components if the mains current as compared to the case with constant $t_{\mu,1}$. The reason is given by the pulsating instantaneous power of a single-phase system loaded with purely sinusoidal current. On the contrary, three-phase systems have a time-constant instantaneous value of power if the mains currents are purely sinusoidal and are in phase with the mains voltages. Therefore one can expect a *reduction* of the mains current harmonics for control method III. The distortion of $i_{N,(RST)}$ which remains to a reduced degree also for constant $p_{O,avg}$ is given by the instantaneous reactive input power [12] required for the system function. For the sake of brevity this shall not be treated here in detail.

In the following analytical approximations are given for the time behavior of $i_{N,(RST)}$ for the control methods described. The calculated current shapes are shown graphically in connection with the numerically gained low-frequency harmonics in dependency on M (cf. **Fig.6**).

5.1 Control Method I

For the shape of the phase current $i_{N,R}$ we receive with Eqs.(1, (2) and section 4 for constant $t_{\mu,1}$ and constant f_P (or constant δ_P):

$\varphi_N \in [0, \frac{\pi}{6}]$:

$$i_{N,R,\tau} = \frac{\sqrt{3}}{4}\delta_P^2 M^{-1}\frac{\cos(\varphi_N) - 2M^{-1}\cos(\varphi_N)\cos(\varphi_N + \frac{\pi}{6}) + \frac{\sqrt{3}}{2}M^{-1}}{(1+\sqrt{3}M^{-1}\sin(\varphi_N - \frac{\pi}{6}))(1 - M^{-1}\cos(\varphi_N - \frac{\pi}{6}))} \tag{22}$$

$\varphi_N \in [\frac{\pi}{6}, \frac{\pi}{3}]$:

$$i_{N,R,\tau} = \frac{\sqrt{3}}{4}\delta_P^2 M^{-1}\frac{\cos(\varphi_N) + \frac{1}{2}M^{-1}\cos(2\varphi_N + \frac{\pi}{6})}{(1-\sqrt{3}M^{-1}\sin(\varphi_N - \frac{\pi}{6}))(1 - M^{-1}\cos(\varphi_N - \frac{\pi}{6}))} \tag{23}$$

$\varphi_N \in [\frac{\pi}{3}, \frac{\pi}{2}]$:

$$i_{N,R,\tau} = \frac{\sqrt{3}}{4}\delta_P^2 M^{-1}\frac{\cos(\varphi_N)}{1-\sqrt{3}M^{-1}\cos(\varphi_N)} \tag{24}$$

The Fourier analysis of the mains current can be performed with the relations given in section 5.4.

The related local mean value $i_{D,avg,\tau}$ oscillating with $6f_N$ (or the related local mean value of the output power $p_{O,avg,\tau} \equiv i_{D,avg,\tau}$) results in:

$$i_{D,avg,\tau}(\varphi_N) = \frac{3}{8}\delta_P^2 M^{-2}\frac{1 - M^{-1}cos(\varphi_N)\cos(2\varphi_N + \frac{\pi}{6})}{(1+\sqrt{3}M^{-1}\sin(\varphi_N - \frac{\pi}{6}))(1 - M^{-1}\cos(\varphi_N - \frac{\pi}{6}))} \tag{25}$$

With good approximation we have:

$$i_{D,avg,\tau} \approx \frac{3}{8}\delta_P^2 \frac{M^{-2}}{1 - M^{-1}\cos(\varphi_N - \frac{\pi}{6})}. \tag{26}$$

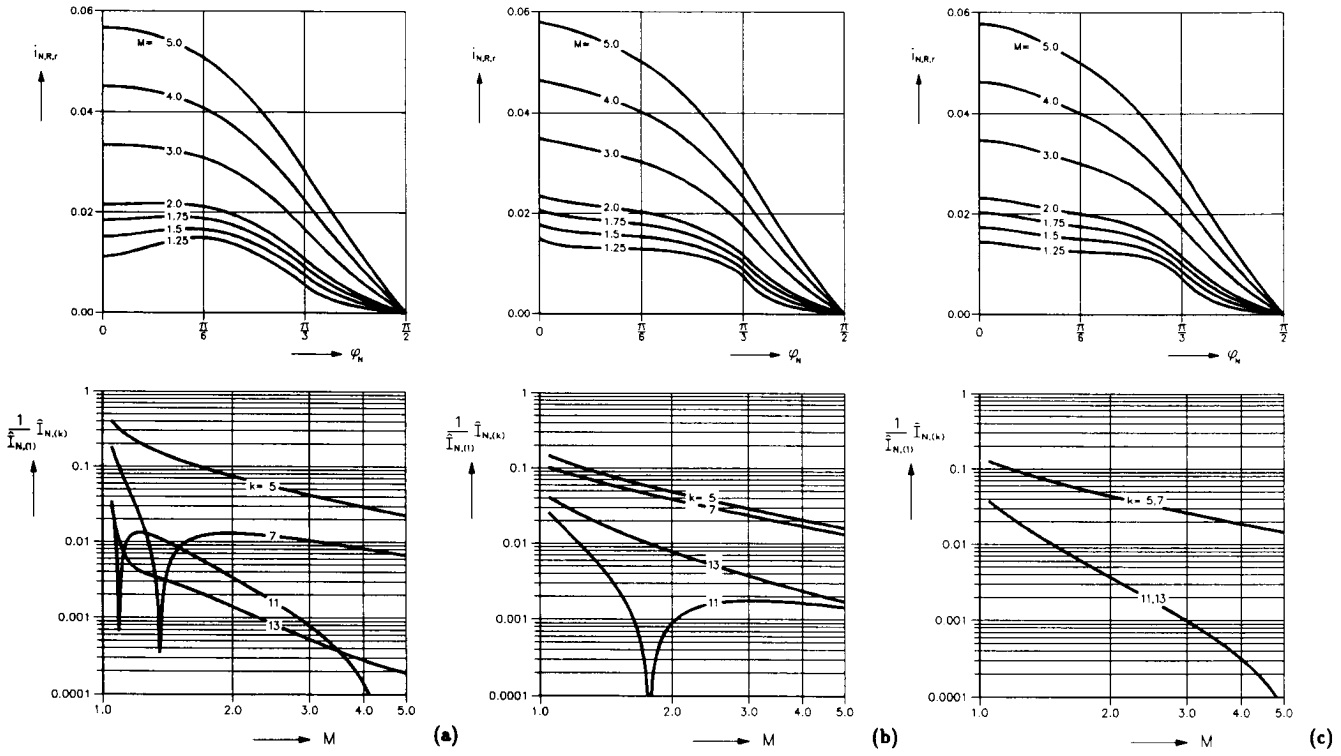

Fig.6: Comparison of different control concepts. Representation of analytically calculated time behaviors (limited to a quarter fundamental period) and of the low frequency mains current harmonics $\hat{I}_{N,(k)}$ referred to the fundamental $\hat{I}_{N,(1)}$ in dependency on M for $P_{O,r} = 0.01$. (a): control method I: f_P and $t_{\mu,1}$ constant over the fundamental period; power pulsations on the DC side due to low frequency harmonics of $i_{N,(RST)}$ are not compensated; the cut-off frequency of the output voltage control loop lies substantially below $6f_N$. (b): control method II: As (a), but f_P not constant. T is turned on immediately after the end of the demagnetisation of L_U at $t_{\mu,3}$; a current gap during $t_\mu \in [t_{\mu,3}, T_P]$ is avoided, the system is operated at the border to continuous mode. (c): control method III: As (a), but $t_{\mu,1}$ not constant. By highly dynamical output voltage control an approximately constant power flow on the DC side is impressed there (constant local mean value $i_{D,avg}$) by appropriate variation of $t_{\mu,1}$. The Fourier coefficients $I_{N,(k)}$ $(k = (5,7);\ (11,13);\ \ldots)$ which lie in the vincinity of the multiples of $6f_N$ show equal amplitude and opposite sign in this case; therefore, they do not occur as harmonics of $i_{D,avg}$ $(\hat{I}_{D,(6i)} \equiv 0, i = 1,2,\ldots)$.

Then, the mean value of $i_{D,avg,r}$ related to the fundamental (or the related output power $P_{O,r} \equiv I_{D,avg,r}$) becomes:

$$I_{D,avg,r} = \frac{1}{2}\delta_P^2\left[\frac{3}{\pi}\Big(\frac{M}{\sqrt{M^2-3}}\Big(\tan^{-1}\frac{\sqrt{3}}{\sqrt{M^2-3}} + \tan^{-1}\frac{\frac{\sqrt{3}-1}{\sqrt{3}+1}M-\sqrt{3}}{\sqrt{M^2-3}}\Big) + \frac{3M}{\sqrt{M^2-1}}\tan^{-1}\frac{\sqrt{3}-1}{\sqrt{3}+1}\sqrt{\frac{M+1}{M-1}} - \frac{\sqrt{3}}{2}M^{-1}\Big) - 1\right]. \quad (27)$$

Approximately we can write

$$I_{D,avg,r} \approx \frac{9}{2\pi}\delta_P^2\frac{M^{-1}}{\sqrt{M^2-1}}\tan^{-1}\frac{\sqrt{3}-1}{\sqrt{3}+1}\sqrt{\frac{M+1}{M-1}}. \quad (28)$$

The equivalent input resistance of the pulse rectifier system defined by Eq.(14) can be calculated according to:

$$R_N = \frac{\pi}{6}\frac{L_U}{T_P}\delta_P^{-2}\sqrt{1-M^{-2}}\left(\tan^{-1}\frac{\sqrt{3}-1}{\sqrt{3}+1}\sqrt{\frac{M+1}{M-1}}\right)^{-1}. \quad (29)$$

R_N is dependent on M due to the duration of the demagnetisation interval being dependent on the difference between input and output voltage (cf. Eq.(20)).

5.2 Control Method II

For the shape of the mains currents we have for turning on T again in $t_{\mu,3}$ (border of discontinuous mode) and for constant $t_{\mu,1}$:

$\varphi_N \in [0, \frac{\pi}{6}]$:

$$i_{N,R,avg,r} = \frac{\sqrt{3}}{4}\delta_P M^{-1}\frac{cos(\varphi_N) - M^{-1}\cos(2\varphi_N + \frac{\pi}{6})}{1+\sqrt{3}M^{-1}\sin(\varphi_N - \frac{\pi}{6})} \quad (30)$$

$\varphi_N \in [\frac{\pi}{6}, \frac{\pi}{3}]$:

$$i_{N,R,avg,r} = \frac{\sqrt{3}}{4}\delta_P M^{-1}\frac{cos(\varphi_N) + \frac{1}{2}M^{-1}\cos(2\varphi_N + \frac{\pi}{6})}{1-\sqrt{3}M^{-1}\sin(\varphi_N - \frac{\pi}{6})} \quad (31)$$

$\varphi_N \in [\frac{\pi}{3}, \frac{\pi}{2}]$:

$$i_{N,R,avg,r} = \frac{\sqrt{3}}{4}\delta_P M^{-1}\frac{cos(\varphi_N) - \frac{1}{2}M^{-1}\sin(2\varphi_N)}{1-\sqrt{3}M^{-1}\cos(\varphi_N)}. \quad (32)$$

According to the system function the averaging of the converter input currents here has to be performed within the interval $t_\mu \in [0, t_{\mu,3}]$ and not within $T_P = \frac{1}{f_P}$. (As opposed to control methods I and III, there is no physical meaning of the frequency f_P which is included in the basis of the normalisation (cf. Eq.(9)).) For the defining equation of the local mean value we have therefore (by modifying Eq.(1)):

$$i_{U,(RST),avg}(\varphi_N) = \frac{1}{t_{\mu,3}}\int_0^{t_{\mu,3}} i_{U,(RST)}(t_\mu)\,dt_\mu. \quad (33)$$

Remark: For single-phase AC-DC boost converters being operated at the border to continuous mode we obtain a purely sinusoidal mains current for constant on-time of the power transistor [13]. In the case at hand there remains a gap $t_\mu \in [t_{\mu,2}, t_{\mu,3}]$ with $i_{U,S} = 0$ (in general, for that current which shows the lowest absolute value at $t_{\mu,1}$, cf. Fig.5, right hand side). This is given despite of the fact that T is switched on again immediately at the end of the demagnetisation (at $t_{\mu,3}$). This gap leads especially in the vincinity of the zero crossings of the mains current to a deviation from a sinusoidal shape (cf. Fig.6). This deviation is characteristic for three-phase single-switch converters. Therefore, low-frequency harmonics occur contrary to the case of the corresponding single-phase system.

The local mean value of the related output power $p_{O,avg,r} \equiv i_{D,avg,r}$ is calculated as

$$i_{D,avg,r} = \frac{3}{8}M^{-2}\delta_P\frac{1 - M^{-1}\cos(\varphi_N)\cos(2\varphi_N + \frac{\pi}{6})}{1+\sqrt{3}M^{-1}\sin(\varphi_N - \frac{\pi}{6})}. \quad (34)$$

A good approximation is given by:

$$i_{D,avg,r} \approx \frac{3}{8} M^{-2} \delta_P \ . \tag{35}$$

Therefore, for the average value of $i_{D,avg,r}$ referred to the fundamental, or for the related output power $P_{O,r} \equiv I_{D,avg,r}$ we receive

$$I_{D,avg,r} = \frac{1}{2}\delta_P^2 \Big[\frac{3}{\pi}\Big(\frac{M}{\sqrt{M^2-3}}(\tan^{-1}\frac{\sqrt{3}}{\sqrt{M^2-3}} + \tan^{-1}\frac{\frac{\sqrt{3}-1}{\sqrt{3}+1}M-\sqrt{3}}{\sqrt{M^2-3}}) + \frac{3M}{\sqrt{M^2-1}}\tan^{-1}\frac{\sqrt{3}-1}{\sqrt{3}+1}\sqrt{\frac{M+1}{M-1}} - \frac{\sqrt{3}}{2}M^{-1}\Big) - 1\Big] \ . \tag{36}$$

According to Eq.(35) one can give the approximation:

$$I_{D,avg,r} \approx \frac{3}{8} M^{-2} \delta_P \ . \tag{37}$$

For the equivalent input resistance R_N we get:

$$R_N \approx 2 \frac{L_U}{T_P} \delta_P^{-1} . \tag{38}$$

Accordingly, R_N is inverse proportional to the relative on-time of T. The output power P_O of the converter then is defined in a first approximation only by the input voltage and $t_{\mu,1}$ contrary to control method I (cf. Eq.(29)). R_N is not dependent on the actual value of U_O.
Remark: Eq.(38) is valid in an analogous manner for the correspondingly controlled DC-DC boost converter where M has to be defined by the ratio of output and input DC voltages.

5.3 Control Method III

For highly dynamical control of the output voltage or for time-constant local mean value $p_{O,avg,r} = P_{O,r}$ or for constant

$$i_{D,avg,r} = P_{O,r} \tag{39}$$

and for constant f_P there follows via Eq.(25) for the relative turn-on time of T:

$$\delta_P^2 = \frac{8}{3} M^2 P_{O,r} \frac{\left(1+\sqrt{3}M^{-1}\sin(\varphi_N - \frac{\pi}{6})\right)\left(1 - M^{-1}\cos(\varphi_N - \frac{\pi}{6})\right)}{1 - M^{-1}\cos(\varphi_N)\cos(2\varphi_N + \frac{\pi}{6})} \tag{40}$$

(δ_P has to be supplied by the controller $R(s)$, cf. Fig.1). A good approximation is given by:

$$\delta_P^2 \approx \frac{8}{3} M^2 P_{O,r} \left(1 - M^{-1}\cos(\varphi_N - \frac{\pi}{6})\right) . \tag{41}$$

The shape of the input current becomes:

$\varphi_N \in [0, \frac{\pi}{6}]$:

$$i_{N,R,avg,r} = \frac{2}{\sqrt{3}} M P_{O,r} \frac{\cos(\varphi_N) - 2M^{-1}\cos(\varphi_N)\cos(\varphi_N + \frac{\pi}{6}) + \frac{\sqrt{3}}{2}M^{-1}}{1 - M^{-1}\cos(\varphi_N)\cos(2\varphi_N + \frac{\pi}{6})} \tag{42}$$

$\varphi_N \in [\frac{\pi}{6}, \frac{\pi}{3}]$:

$$i_{N,R,avg,r} = \frac{2}{\sqrt{3}} M P_{O,r} \frac{\cos(\varphi_N) + \frac{1}{2}M^{-1}\cos(2\varphi_N + \frac{\pi}{6})}{1 + M^{-1}\cos(\varphi_N - \frac{\pi}{3})\cos(2\varphi_N + \frac{\pi}{6})} \tag{43}$$

$\varphi_N \in [\frac{\pi}{3}, \frac{\pi}{2}]$:

$$i_{N,R,avg,r} = \frac{2}{\sqrt{3}} M P_{O,r} \frac{\cos(\varphi_N)\left(1 - M^{-1}\sin(\varphi_N)\right)}{1 - M^{-1}\cos(\varphi_N - \frac{\pi}{3})\sin(2\varphi_N)} \ . \tag{44}$$

For R_N we receive directly with Eqs.(10 and 14):

$$R_N = \frac{3}{4} \frac{L_U}{T_P} M^{-2} P_{O,r}^{-1} . \tag{45}$$

5.4 Fourier Analysis

According to the chosen position of the starting point $\varphi_N = 0$ of the phase angles within the fundamental and to the assumptions regarding symmetry (cf. section 3.1) there follow the Fourier coefficients of the mains current via:

$$I_{N,(k),r} = \frac{4}{\pi} \int_0^{\frac{\pi}{2}} i_{N,r}(\varphi_N)\cos(k\varphi_N)\, d\varphi_N \qquad k = 1,5,7,11,13\ldots \ . \tag{46}$$

For the amplitudes of the mains current harmonics we have:

$$\hat{I}_{N,(k),r} = |I_{N,(k),r}| \ . \tag{47}$$

The related fundamental of the mains current can be given directly by rating of the power balance equation Eq.(13) via:

$$\hat{I}_{N,(1),r} = \frac{2}{\sqrt{3}} M P_{O,r} \ . \tag{48}$$

5.5 Mains Filter

For the sake of brevity only a few important points for dimensioning of the mains filter (shown in Fig.1 as simple single-stage type L_N, C_N) are given.

In general, dimensioning of L_N, C_N has to be performed such that the high frequency harmonics of $i_{U,(RST)}$ are suppressed and that an increase of the low frequency harmonics is avoided. Therefore, the low frequency harmonics of $i_{U,(RST)}$ basically are not influenced by the mains filter. They occur directly as mains current harmonics. Furthermore, the danger of excitation of the filter by ripple-control signals ($f < 1.4$kHz) has to be observed. The filter resonance frequency therefore has to be selected above $50 f_N$. According to VDE 0871, the required damping at switching frequency has to be > 80dB for systems with output powers in the kW region. Due to this the filter has to be designed as a higher order type (e.g., 3 LC-stages) and a switching frequency $f_P > 500 f_N$ is required. One has to keep in mind, however, that for a number of stages > 3 further stages contribute only to a relatively small degree to the overall damping. More than one stage is also to be favored regarding the decreasing sensitivity of the filter characteristic with respect to the inner mains impedance. As, e.g., described in [14] and [15], for high dynamics of the voltage control loop one also has to include the input filter transfer function into the controller design.

Dimensioning of the filter with optimal damping and minimum weight and size in general is a very important aspect for the practical applicability of the system. This also is especially true because (as already evident by the high required damping) inclusion of volume and weight of the filter cuts the power density of the rectifier into about one half as compared to the case without filter. Therefore, also the filter cost will have a substantial influence on the overall system cost.

A reduction of the filtering effort can be achieved only by increasing f_P. Connected herewith, the extension of three-phase single-switch discontinuous-mode boost rectifiers to quasi-resonant operation (as discussed in [8]) seems to be of special importance. An alternative to increasing f_P is given by paralleling of several systems which are pulsed with shifted phases. This method becomes economically interesting only for higher output power, however.

5.6 Comparison of the Control Methods

As the comparisons given in Fig.6 makes clear, all control methods show a quality of the mains current being significantly dependent on M.

For $M > 5$ we have approximately purely sinusoidal current shape (or a shape proportional to the mains voltage, respectively). Due to U_O being relatively high compared to $\sqrt{3}\hat{U}_N$ the demagnetization of L_U will need only a minor part of the pulse period. The current rise being proportional to $u_{N,(RST)}$ within $t_\mu \in [0, t_{\mu,1}]$ therefore leads to local mean values $i_{U,(RST),avg}$ being also largely proportional to $u_{N,(RST)}$. This means also an approximate voltage-proportional shape of the mains currents $i_{N,(RST)}$. Generally, one has to strive for U_O as high as possible therefore.

Due to $U_O = 660\text{V}\ldots 820\text{V}$ being present for an operation of the system in the European mains especially $M < 1.5$ is of interest for a practical realisation. For constant f_P and high dynamics of the control of u_O (control method III, cf. (c) in Fig.6) we obtain a reduction of the 5th harmonic of $i_{N,(RST)}$ in the region $M < 2.0$ as compared to the operation with constant $t_{\mu,1}$ (control method I, cf. (a) in Fig.6). However, this is connected with an increase of the 7th harmonic. When the system operates at the border of the discontinuous mode (control method II) there occurs a modulation of the duty cycle of T which is comparable to that given for constant $p_{O,avg}$ (cf. Fig.7, (b) and (c)). This results in an approximately similar shape of the dependency of the 5th and 7th harmonic on M (cf. Fig.6, (b) and (c)).

For $M < 1.25$ especially for control method I high amplitudes of the low frequency harmonics of $i_{N,(RST)}$ occur. There, the current shape within a pulse period and the local current mean value are mainly determined by the demagnetisation phase. Due to the only low difference between peak value of the line-to-line voltages and U_O the relative duration of the second part $t_\mu \in [t_{\mu,2}, t_{\mu,3}]$ of the demagnetisation interval is substantially increased as compared to higher U_O. This results in a wide gap for that phase current which shows the smallest absolute value in $t_{\mu,1}$. This gap finally causes the distortion of $i_{N,(RST)}$. Furthermore, in this region of operation an extremely low utilisation factor of T has to be observed. The converter application

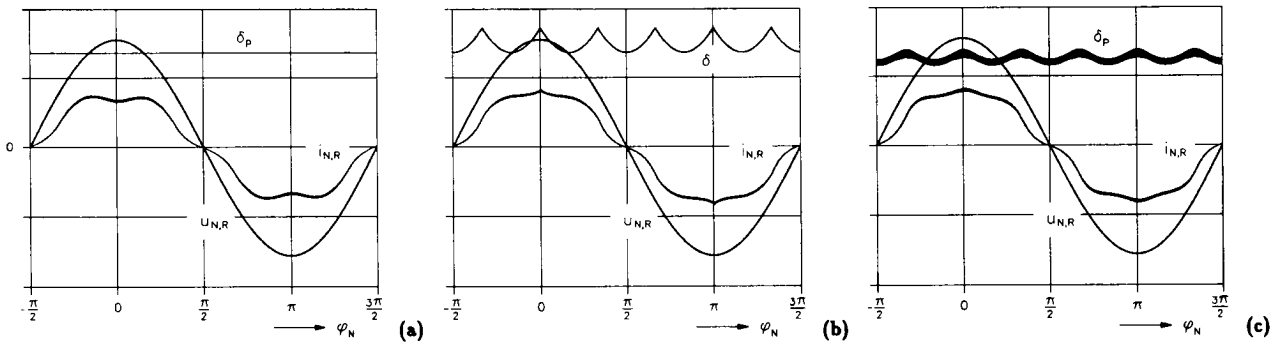

Fig.7: Comparison of different control concepts by digital simulation of the system; ideal system components are assumed; representation of the mains phase voltage $u_{N,R}$ (200V/div), of the related mains current $i_{N,R}$ (20A/div); furthermore representation of: relative turn-on time δ_P of T (for control method I and III) and the quantity δ corresponding to the local switching frequency for control method II (cf. Eq(21)), 0.5/div; parameters: $U_{N,rms}$ =220V, U_O =820V ($M \approx 1.5$), f_N =50Hz, f_P = 45kHz, $L_U = 75\mu$H, $L_N = 250\mu$H, $C_N = 2.5\mu$F, C =4.0mF; **(a): Control Method I**: pulse frequency f_P and turn-on time of the power transistor $t_{\mu,1} = 7.6\mu$s constant over the fundamental period, C =4mF, P_O=6.875kW; **(b): Control Method II**: operation at the border of the discontinuous mode for constant turn-on time $t_{\mu,1} = 7.6\mu$s, C =4mF, P_O=7.5kW; **(c): Control Method III**: highly dynamical control of the output voltage for constant pulse frequency f_P, P-controller: $R(s) = k_P$, zero-crossing frequency of the voltage control loop: f_O =1.025kHz, C =1.0mF, P_O=7.5kW.

therefore has to be limited to $U_O > 3.0\ U_{N,rms}$ independent of the selected control method.

6 Digital Simulation

The comparison of the results of the theoretical analysis performed in the previous section with a digital simulation (cf. **Fig.7**) shows that the deviations are less than 1% for $f_P \geq 500 f_N$. According to the assumtions of the analytical calculation ideal system behavior is also assumed for the digital simulation. Relative quantities like the mains current harmonics (rated to the fundamental) are influenced only in a very slight manner by these neglections. Therefore, the results of the analytical calculation allow a very accurate judgement of the mains behavior of the system.

Besides the shape of mains voltage $u_{N,R}$ and mains current $i_{N,R}$ Fig.7 also represents the relative turn-on time δ_P (for control method I and II; cf. Fig.7 (a) and (c)) and the ratio $\delta = t_{\mu,1}/t_{\mu,3}$ which characterizes the time shape of the local pulse frequency given for control method II (cf. Fig.7, (b)).

Because the current gap $t_\mu \in [t_{\mu,3}, T_P]$ is avoided if the system is operated at the border to continuous mode, for equal turn-on time $t_{\mu,1}$ control method II leads to an increased output power P_O as compared to constant f_P (control method I). In general, a relatively small additional effort regarding the converter control circuit results in a better utilisation of the components of the power circuit. Nevertheless it has to be kept in mind that this operating mode leads to very high switching frequencies in the region of small output power. Therefore, a pulse frequency limitation has to be provided especially for systems with high rated power.

Figure 7 (c) shows the relationships for highly dynamic output voltage control. Besides the control error the controller $R(s)$ also amplifies the voltage ripple of the output capacitor C. This leads for a given zero-crossing frequency of the open loop gain to a relatively wide high-frequency variation of the turn-on time which is approximately independent of the capacitance value of C. For a practical realisation a proper measurement filter has to be used, e.g., a measuring system which averages u_O over a pulse period.

7 Experimental Results

As can be seen clearly from comparing Figs. 6 and 8, the theoretical considerations are consistent with the measurements on a laboratory model. For the sake of brevity, the representation of the measurements is limited to the converter operation with constant $t_{\mu,1}$ and constant f_P (control method I).

For minimising the system cost one has to investigate the possibility to realise the three-phase diode bridge as rectifier module. **Figure 8 shows** the situation for using such a module and for using discrete diodes with low reverse recovery time arranged as a three-phase bridge.

Due to the high reverse recovery time we experience a distortion of the diode bridge input currents, e.g., of $i_{U,R}$ (cf. Fig.8, (a)) if a rectifier module is applied. For high-speed diodes (cf. Fig.8, (b)) we have approximately ideal conditions. $i_{N,R}$ shows almost identical shape in both cases. The distortion of $i_{U,R}$ is limited to intervals of $\frac{\pi}{3}$ located symmetrical to the zero crossings of $i_{N,R}$. This can be explained by the fact that in this region a higher rate of decay of the current $i_{U,R}$ is encountered than in the rest of the mains period. In general, a higher rate of decay at the zero crossings of the input currents $i_{U,(RST)}$ is given for that phase which shows the smallest absolute current value at $t_{\mu,1}$. As shown in section 4 for $\varphi_N \in [0, \frac{\pi}{6}]$, only the projection of $\underline{u}_N - \underline{u}_{U,[100]}$ is effective after the end of the first phase of demagnetisation in $t_{\mu,2}$ (cf. Fig.5). Therefore, the zero crossings of $i_{U,R}$ and $i_{U,T}$ in $t_{\mu,3}$ shows a smaller rate of decay than that of $i_{U,S}$ in $t_{\mu,2}$. For higher switching frequency the current distortion can be experienced to a higher degree also in the other regions of φ_N. Therefore, the diode bridge has to be realised with discrete semiconductors also because the diode losses would rise significantly.

8 Conclusions

As this paper shows, the effect on the mains of a three-phase single-switch discontinuous-mode boost rectifier system is essentially determined by the voltage transformation ratio and by the dynamics of the output voltage control. One has to point out that the results of the converter analysis given in

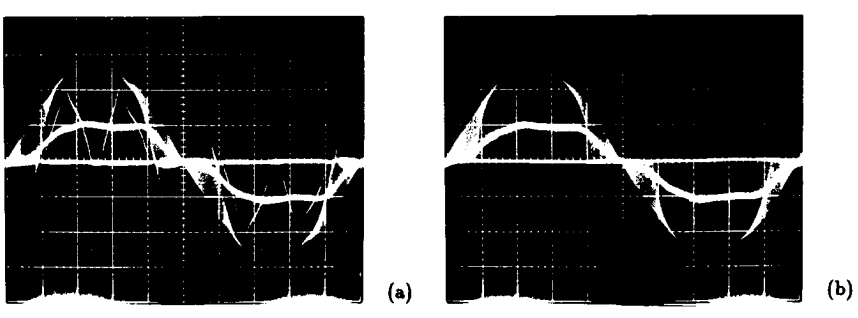

Fig.8: Measurements on a 2.5kW laboratory model of a three-phase single-switch discontinuous-mode boost rectifier; time behavior of the input current $i_{U,R}$ of the three-phase diode bridge and of the related mains phase current $i_{N,R}$ for control method I (constant $t_{\mu,1}$ and constant f_P); 10A/div; parameters: M = 1.5, $U_{N,rms}$ = 115V,, f_N = 50Hz, f_P = 10.05kHz, L_U = 75μH, single stage filter: L_N = 1.2mH, C_N = 22μF, P_O = 2.5kW, realisation of the diode bridge: **(a):** by using a three-phase rectifier module; **(b):** application of discrete diodes with low reverse recovery time arranged as three-phase bridge.

this paper can be applied directely to the assessment of the mains behavior of a three-phase single-switch Ćuk rectifier [8], [9] and of further converters with equal structure of the input section [8].

In connection with the limitation of the harmonics stress on public mains (as enforced by regulations and standards) three-phase single-switch pulse rectifiers will gain increased importance in the future because of the simple structure of the power and control circuit. For industrial application of the converter especially the optimal dimensioning of the mains filter will be of importance. This is also true for the minimisation of the increase of the input current distortion occurring for mains unsymmetries. Related investigations are the topic of further research at present.

ACKNOWLEDGEMENT

The authors are very much indebted to the Austrian **Fonds zur Förderung der wissenschaftlichen Forschung** which supports the work of the Power Electronics Section at their university.

References

[1] **Prasad, A.R., Ziogas, P.D., and Manias, S.:** *An Active Power Factor Correction Technique for Three-Phase Diode Rectifiers.* IEEE Transactions on PE, Vol.6, No.1, pp. 83–92 (1991).

[2] **Mohan, N., Undeland, T.M., and Robbins, W.P.:** *Power Electronics: Converters, Applications, and Design.* New York: John Wiley & Sons (1989).

[3] **Liu, K.H., and Lin, Y.L.:** *Current Waveform Distortion in Power Factor Correction Circuits Employing Discontinuous-Mode Boost Converters.* Conference Record of the 20th IEEE PESC, Milwaukee, June 26–29, Vol.II, pp. 825–829 (1989).

[4] **Kolar, J.W., Ertl, H., and Zach, F.C.:** *Calculation of the Passive and Active Component Stress of Three-Phase PWM Converter Systems with High Pulse Rate.* Proceedings of the 3rd European Conference on Power Electronics and Applications, Aachen, Oct. 9-12, Vol.3, pp. 1303–1311 (1989).

[5] **Erickson, R., Madigan, M., and Singer, S.:** *Design of a Simple High-Power-Factor Rectifier Based on the Flyback Converter.* Conference Record of the 5th IEEE APEC, Los Angeles, March 11–16, 792–801 (1990).

[6] **Jardan, K.R., Dewan, S.B., and Slemon, G.R.:** *General Analysis of Three-Phase Inverters.* IEEE Transactions on Industry and General Applications, Vol. IGA-5, No.6, pp.672–679 (1969).

[7] **Singer, S., and Erickson, R.W.:** *Canonical Modeling of Power Processing Circuits Based on the POPI Concept.* IEEE Transactions on PE, Vol.7, No.1, pp.37–43 (1992).

[8] **Ismail, E., and Erickson, R.W.:** *A Single Transistor Three-Phase Resonant Switch for High-Quality Rectification.* Conference Record of the 23rd IEEE PESC, Madrid, June 29–July 3, Vol.II, pp. 1341–1351 (1992).

[9] **Malesani, L., Rossetto, L., Spiazzi, G., Tenti, P., Toigo, I., and Dal Lago, F.:** *Single-Switch Three-Phase AC-DC Converter with High Power Factor and Wide Regulation Capability.* Proceedings of the 14th IEEE INTELEC, Washington, D.C., Oct. 4–8, pp. 279–285 (1992).

[10] **Lin, F., and Chen, D.Y.:** *Reduction of Power Supply EMI Emission by Switching Frequency Modulation.* Proceedings of the 10th Annual VPEC Power Electronics Seminar, Blacksburg, VA, Sept. 20-22, pp. 129–136 (1992).

[11] **Takahashi, I., and Itoh, Y.:** *Electrolytic Capacitor-Less PWM Inverter.* Proceedings of the International Power Electronics Conference, Tokyo, April 2-6, Vol.1, pp. 131–138 (1990).

[12] **Akagi, H., Kanazawa, Y., and Nabae, A.:** *Generalized Theory of the Instantaneous Reactive Power in Three-Phase Circuits.* Proceedings of the International Power Electronics Conference, Tokyo, March 27–31, Vol.2, pp. 1375–1386 (1983).

[13] **Schott, W., and Herfurth, M.:** *Switched Mode Power Supply with Power Factor Correction.* Proceedings of the 6th International Conference on Power Electronics and Motion Control, Budapest, Oct. 1-3, Vol.2, pp. 64–68 (1990).

[14] **Lee, F.C., and Yu, Y.:** *Input Filter Design for Switching Regulators.* IEEE Transactions on Aerospace and Electronic Systems, Vol.AES-15, No.5, pp. 627–634 (1979).

[15] **Kislovski, A.S., Redl, R., and Sokal, N.O.:** *Dynamic Analysis of Switching-Mode DC/DC Converters.* New York: Van Nostrand Reinhold (1991).